# Physics of U.S. surface temperature response to ENSO forcing

**Tao Zhang, Martin P. Hoerling, Judith Perlwitz,**

**De-Zheng Sun, and Don Murray**

**Cooperative Institute for Research in Environmental Sciences**

**University of Colorado/NOAA Earth System Research Laboratory**

**Physical Sciences Division**

**Boulder, Colorado**

(*Submitted to Journal of Climate*)

July 23, 2010

*Corresponding author address:* Dr. Tao Zhang, 325 Broadway, R/PSD1, CIRES and NOAA/PSD, Boulder, CO 80305. Email: tao.zhang@noaa.gov

## Abstract

In order to elucidate physical processes responsible for the U.S. response to ENSO, the surface energy balance is diagnosed with emphasis on the role of clouds, water vapor, and land surface properties associated with snow cover and soil moisture. Results for the winter season (December, January, February) indicate that U.S. surface temperature conditions associated with ENSO are determined principally by anomalies in the surface radiative heating—the sum of absorbed solar radiation and downward longwave radiation. Each component of the surface radiative heating is linked with specific characteristics of the atmospheric hydrologic response to ENSO, and also to feedbacks by the land surface response. During El Niño, surface warming over the northern U.S. is physically consistent with three primary processes: i) increased downward solar radiation due to reduced cloud optical thickness, ii) reduced reflected solar radiation due to an albedo decline resulting from snow cover loss, and iii) increased downward longwave radiation linked to an increase in precipitable water. Southern U.S. coolness during El Niño is mainly the result of a reduction in incoming solar radiation resulting from increased cloud optical thickness. During La Niña, most of the U.S. warms during winter. Across the central U.S., a warming contribution mainly stems from snow cover losses, whereas Southern U.S. warming results from a reduction in cloud optical thickness associated with increased incoming solar radiation. Our results advance understanding of the factors responsible for the U.S. response to ENSO forcing, and may be useful for assessing the strengths and limitation of climate models utilized in seasonal predictions and projections, and for attribution of the physical causes for climate variability and change.

## 1. Introduction

El Niño-Southern Oscillation (ENSO) induces a strong natural interannual climate signal that affects the surface climate in numerous regions of the globe including the continental United States. The effect of ENSO on the U.S. surface temperature has been documented in many previous studies (Ropelewski and Halpert, 1986, 1987; Kiladis and Diaz 1989; Hoerling et al. 1997; Larkin and Harrison 2005; Wang et al. 2007; Lau et al. 2008). During El Niño winter, the northern contiguous United States is dominated by warm temperature anomalies and the southern United Sates is dominated by cold temperature anomalies. During La Niña winter, there is a general reversal in temperature anomalies in many regions of the United States, though the response is not strictly linear (e.g. Hoerling et al. 1997). Despite the strong impact of ENSO on U.S. climate and even though it is widely recognized to provide the principal source of seasonal forecast skill for the U.S. (e.g. Quan et al. 2006), little is known about the physical processes responsible for the surface temperature signals. Virtually all of ENSO-impact studies have focused on atmospheric teleconnections (e.g. Trenberth et al. 1998; Hoerling and Kumar 2000), but these alone can not explain the immediate causes for the surface temperature anomalies.

It is understood that the tropical SST anomalies excite the propagation of Rossby waves from the tropical Pacific polewards and eastwards to the Americas and thereby affect the region's climate (see review by Trenberth et al. 1998). Such circulation changes will also modify water vapor and clouds over the Americas, though these latter attributes of the teleconnection processes have not been well described, nor is the impact of the

hydrologic cycle on surface energy balances during ENSO well understood. According to the first law of thermodynamics ($\frac{\partial T}{\partial t} = -\vec{V} \cdot \nabla T - \omega \frac{\partial T}{\partial p} + \frac{\alpha}{C_p}\omega + \frac{\dot{q}}{C_p}$), the time tendency of surface temperature (left-hand side term) is determined by diabatic heating (the last right-hand side term), because the horizontal advection of temperature, the vertical advection of temperature and the adiabatic heating terms are negligible at the surface. The diabatic heating is intimately tied to the hydrological cycle including the radiative effects of water vapor and clouds and changes in surface properties such as soil moisture and snow cover.

As an essential component of the global hydrologic cycle, water vapor and clouds contribute significantly to Earth's climate (e.g. Chahine 1992; Ramanathan et al. 2001; Sun et al. 2003). While extensive efforts has been devoted to assessing the changes in the hydrologic cycle associated with ENSO over the oceans (Soden 2000; Sun et al. 2003, 2006, 2009; Zhang and Sun 2006, 2008), less attention has been given to describing the changes in the hydrologic cycle over land, especially over the continental United States. Yang et al. (2001) studied the impact of snow variability induced by ENSO on surface temperature responses over the North America. They argued that the snow-albedo feedback is an important factor in affecting the North America surface climate anomaly. The importance of snow-albedo feedback highlighted in their study addresses the role of one component of local surface diabatic heating—the upward shortwave radiative flux at surface. However, there is limited understanding of the role of water vapor and clouds which control the downward longwave and downward shortwave radiative fluxes, respectively. It is the interplay between these various components of surface diabatic

heating that are coupled through the hydrologic cycle, and further coupled with the large-scale atmospheric dynamics, that determine the surface temperature response to ENSO over the United States.

The purpose of this paper is to understand the physics of U.S. surface temperature response to ENSO forcing by highlighting the role of water vapor and clouds. We organize this paper as follows. Section 2 describes the methodology of our analysis and the observational datasets used in this study. Section 3 presents the observed response of U.S. surface temperature to El Niño and La Niña, and then investigates the responses of surface energy components to identify the major physical factors determining the U.S. surface temperature response. The relative roles of water vapor, clouds and snow cover are examined in order to understand the response of the various surface energy fluxes. We find that the U.S. surface temperature response to ENSO is mainly determined by anomalies in the surface radiative heating defined as the sum of absorbed solar radiation and downward longwave radiation. Water vapor and cloud changes play a key role in the U.S. surface temperature response by regulating the downward longwave radiation and downward solar radiation, respectively. Further, the snow-albedo feedback is also an important factor in determining the U.S. surface temperature response via its impact on upward shortwave radiation. A summary of principal results is given in section 4.

## 2. Methodology and Data

The change in surface energy components is subject to the law of energy conservation and therefore the sum of the change in various components must be equal to zero. Wild et

al. (2004) give a detailed equation of surface energy balance,

$$\Delta SW_{absorbed} + \Delta LW_{down} + \Delta LW_{up} + \Delta SH + \Delta LH + \Delta GH + \Delta M = 0 \quad (1)$$

where $SW_{absorbed}$, $LW_{down}$, and $LW_{up}$ are the absorbed shortwave radiative flux at surface, downward and upward longwave radiative fluxes at surface, respectively, $SH$ and $LH$ are the sensible and latent heat fluxes, $GH$ is the ground heat flux and $M$ is the energy flux used for melt.

As demonstrated by Wild et al. (2004), the last two terms ($\Delta GH$ and $\Delta M$) are very small, thus the equation for the changes in surface energy balance can be written as

$$\Delta SW_{absorbed} + \Delta LW_{down} + \Delta LW_{up} + \Delta SH + \Delta LH = 0 \quad (2)$$

The sum of the absorbed shortwave and downward longwave radiation fluxes (the first two terms of Equation (2)) is defined as the surface radiative heating, which indicates the radiative energy input to the surface. In response to the imposed change of surface radiative heating, the surface redistributes the changed energy content among the nonradiative fluxes of the surface energy balance ($SH$ and $LH$) and the surface longwave emission ($LW_{up}$).

In the present study, we will focus on the impact of ENSO on the U.S. hydrologic cycle during Northern winter (December to February) using multiple observational datasets. We will conduct composite analysis to understand coherent features in the response of the hydrologic cycle to El Niño and La Niña SST forcing over the continental United States. The definition of warm and cold events is based on the same method as used by Hoerling et al. (1997), and the warm and cold event years used in the composite (see

Table 1) are selected due to the availability of the satellite data from which to determine the surface energy balance.

The ISCCP (International Satellite Cloud Climatology Project) FD data (Zhang et al. 2004) and ISCCP D2 data (Rossow et al. 1996) will be used for examining the response of water vapor and clouds over the U.S. to ENSO forcing, respectively. The ISCCP FD data also include the monthly radiative fluxes both at surface and at the top of the atmosphere (TOA), which allows us to perform the surface energy budget analysis. The corresponding surface latent and sensible heat fluxes are obtained from ERA-40 reanalysis (Uppala et al. 2005). For consistency, the surface temperature data from ISCCP FD data sets are also used in this study. We will examine the responses of snow cover and soil moisture from NARR data (Mesinger et al. 2006) to infer features of land surface wetness over the continental United States. We will also examine the CMAP precipitation (Xie and Arkin 1997) data to infer soil moisture conditions.

## 3. Results

The wintertime patterns of the surface temperature anomalies observed during El Niño and La Niña are displayed in the top and bottom panels of Figure 1, respectively. During El Niño, maximum warm temperature anomalies are located over western Canada and the northern U.S., while the surface temperature is colder than the normal over the southern tier of states and the East (Fig.1a). These key features agree well with the previous

observational findings based on larger sample sizes (e.g. Hoerling et al. 1997; Larkin and Harrison 2005; Lau et al. 2008).

There is a general reversal in the pattern of surface temperature anomalies during La Niña, with the cold (warm) anomalies prevailing in the northwest (southeast) of the North American landmass (Fig.1b). The present composites for ENSO events after 1986 show an asymmetry in temperature anomalies over the northern regions of U.S. (about poleward of 37$^{o}$N), where strong warm anomalies occur during both El Niño and La Niña events, consistent with a nonlinearity in ENSO teleconnections reported in Hoerling et al. (1997).

Anomalies in the individual components of the surface energy balance are shown for El Niño (left column of Figure 2) and for La Niña (right column of Figure 2). We adopt a sign convention in which contributions to positive (negative) local temperature tendency are plotted in red (blue). Regarding the effect of changes in the upward longwave radiation, it represents simply a response to the anomalous surface temperature itself following the Stefan-Boltzmann law. Thus, temperature tendencies induced by upward longwave flux anomalies are out-of-phase with the composite surface temperature anomalies (compare Figure 1 with top panels of Figure 2).

The surface radiative heating, defined as the sum of absorbed surface net shortwave radiation flux and the downward surface longwave radiation flux, provides a more insightful indication of how water vapor and cloud feedbacks determine the U.S. surface

temperature response to ENSO. It is clear from the second row panels in Figure 2 that the patterns of observed temperature anomalies during El Niño and La Niña are almost entirely determined by the surface radiative heating. Note that the large positive anomalies of surface radiative heating over the northern U.S. agree well with the strong warm temperature anomalies over that region, and the small negative anomalies of surface radiative heating over the southern U.S. are also in accord with the weak cold temperature anomalies over that region (Fig.2b and Fig.1a). The change in the surface net radiation, which is the sum of the anomalous upward surface longwave radiation and anomalous surface radiative heating, is a small residual resulting from a cancellation of these two components. We use the ERA-40 reanalysis to estimate the composite anomalies for sensitive and latent heating, the results of which are shown in the lower panels of Figure 2. Despite the independent sources of information for the radiative and turbulent heat fluxes, a broad compensation between net surface radiation and turbulent heat fluxes (LH+SH), as demanded by Equation (2), is evident.

The role of clouds, water vapor and land surface feedbacks in determining the pattern of U.S. surface temperature anomalies during ENSO can be inferred from a diagnosis of the two components of surface radiative heating—the absorbed shortwave radiation and the downward longwave radiation. Figure 3 shows the response of the absorbed shortwave radiation (top row), which is the sum of the reflected (upward) surface shortwave radiation (second row) and the incident downward shortwave radiation (third row). During El Niño winters, a warming contribution due to increased absorbed solar radiation over the northwestern U.S. is the result of two physical processes: a reduction in

surface albedo due to snow cover loss (see Figure 4) and increased incoming solar radiation due to a reduction in cloud optical thickness (Figure 3, bottom). During La Niña winters, a contribution to cooling by the reduction in absorbed shortwave radiation over the far Northwest U.S. (Figure 3, top right) is mainly the result of increased cloud optical thickness (Figure 3, bottom right). Over the Southern U.S., a cooling (warming) during El Niño (La Niña) by the decreased (increased) absorbed shortwave radiation is mainly due to the increase (reduction) in cloud optical thickness. Interestingly, the total cloud cover appears to be not the major contributor to the response of incoming solar radiation over the United States during ENSO, since the pattern of changes in total cloud cover does not correlate with that of surface incoming solar radiation over most regions except the northwest and southwest (not shown).

The response of land surface properties to the different phases of ENSO forcing is an important element in understanding the land surface temperature responses themselves, and also in understanding the asymmetry of those responses between El Niño and La Niña (see Figure 1). A key feature is the general decrease in surface albedo over the U.S. during both phases of ENSO (Figure 4, top). This is largely related to snow cover reduction over the northern-central U.S. during El Niño, and mainly over the central U.S. during La Niña (Figure 4, second row). When marginally snow covered areas are initially warmed, for example, through increased downward shortwave radiation (see Figure 3) or increased downward longwave radiation (see Figure 5), snow is apt to melt, lowering the albedo which in turn can cause a positive temperature-snow feedback. Soil moisture changes associated with precipitation anomalies (lower rows of Figure 4)

appear to play a role in the surface temperature response through effects on surface albedo also. Increased (decreased) surface albedo over the Southern U.S. is associated with increased (decreased) precipitation and soil moisture during El Niño (La Niña). It is unclear how these soil moisture anomalies may have induced the local surface albedo changes, however, because the relationship implied in Figure 4 appears contrary to the observational indication that sand and soils exhibit reduced albedo when wet (e.g. Twomey et al. 1986).

The other key radiative forcing that determines the land surface temperature response to ENSO is the anomalous downward longwave radiation (Figure 5, top). In several areas of the U.S., its amplitude exceeds that of the anomalous absorbed shortwave radiation (see Figure 3, top), most notably in vicinity of the Canadian border, and also over the Southwest U.S. during La Niña. Changes in atmospheric water vapor content are the principal source for the anomalous downward longwave radiation, as is readily apparent from the very close spatial agreement between the anomalous precipitable water (Figure 5, bottom) and the downward longwave radiation (Figure 5, top). During El Niño, an almost continent-wide increase in atmospheric water vapor contributes to an elevated greenhouse effect (e.g. Zhang and Sun 2008) and a forcing of surface temperature warming through the resulting change in downward longwave radiation. Note once again that the anomalous longwave forcing of surface temperature during El Niño is not equal and opposite to that during La Niña, thus further contributing to the asymmetry in the respective surface temperature response above and beyond that resulting from snow-albedo feedbacks.

It is also interesting to see that the pattern of precipitable water change is mostly opposite to the change in precipitation itself (see Figure 4, bottom). Areas of increased (reduced) total column water vapor generally experience reduced (increased) winter precipitation, suggesting that the mechanism for precipitation responses to ENSO is intimately linked to the dynamics of weather systems, frontal boundaries, and the phenomena responsible for inducing adiabatic vertical motions and mass convergence, and not merely to the water vapor abundance itself.

## 4. Summary and discussion

An analysis of surface energy budget was presented in order to identify the major contributors to the U.S. surface temperature anomalies during ENSO. The study focused on the responses of water vapor, clouds and land surface properties in order to provide an understanding of the physical processes that shape the regional U.S. wintertime surface temperature anomaly patterns during El Niño and La Niña.

The surface energy balance requires that the change in surface radiative heating (defined as the sum of absorbed solar radiation and downward longwave radiation) must be balanced by the upward longwave radiation and the net turbulent flux (the sum of latent and sensible heat fluxes). Over land in particular, the change in surface radiative heating is the dominant physical mechanism for determining the response of U.S. surface temperature. As a summary of the physical processes associated with the U.S. ENSO response, Table 2 presents the principal radiative forcings averaged geographically over

the largest surface temperature signals. During El Niño, strong northern U.S. warming and Gulf Coast cooling result from increased and reduced surface radiative heating, respectively. The former warming is mainly attributed to increased downward longwave radiation and a reduced reflection of solar radiation which are linked to increased precipitable water and decreased snow cover, respectively. The latter Gulf Coast cooling is mainly due to the reduction in incident solar radiation resulting from increased cloud optical thickness. During La Niña, strong central and southern U.S. warming likewise results from increased surface radiative heating. Warming over the central U.S. is largely determined by a reduced reflection of solar radiation, owing to snow cover loss. Warming over the Gulf Coast is mainly due to increased incident solar radiation associated with reduced cloud optical thickness, and also due to increased downward longwave radiation associated with a column increase in precipitable water.

Figure 6 further summarizes our principal findings via a schematic of the main physical processes that explain the U.S. surface temperature responses to ENSO forcing. The diagram highlights the interplay among various features of the hydrological cycle and their ultimate effects on surface temperature. In particular, our analysis reveals that the patterns of surface albedo and cloud optical thickness change are highly congruent, and that each further linked to patterns of anomalous precipitation. During El Niño, dynamical processes tied to storm track shifts (e.g. Hoerling and Ting 1994; May and Bengtsson 1998) result in below normal precipitation over the northern and western U.S. (see Figure 4), and the implied reduced upward vertical motion results in reduced cloud optical thickness, acting to warm surface temperature. This radiatively forced warming

combines with reduced precipitation to reduce snow cover over the same region, thereby acting to amplify the surface warming. A similar interplay of physical processes occurs across the central U.S. during La Niña. Precipitation is broadly reduced over the central Great Plains as the storm track shifts northward to the Canadian border (e.g. Held et al. 1989), leading to reduced upward motion and reduced cloud optical thickness. The resultant surface warming is amplified by a resulting loss in snow cover. The pattern of precipitable water, which further drives surface temperature through water vapor feedbacks, is largely in phase with the overall temperature anomaly itself. During El Niño, greater (lesser) atmospheric water vapor content over the northern (southern) U.S. is consistent with a vertically averaged tropospheric warming (cooling) associated in part with anomalous descent (ascent). These regions of tropospheric warming (cooling) have greater (lesser) water holding capability. A similar argument pertains to the relation between column precipitable water and atmospheric dynamics during La Niña. There is thus a strong coupling between downward longwave radiative flux, as implied by the sign of precipitable water anomalies, and the dynamically driven changes in precipitation itself. In total, based on diagnosis of both shortwave and longwave radiation, our analysis of the physical processes responsible for the U.S. surface temperature response to ENSO indicates a strong link with dynamical processes that determine vertical motion and precipitation.

Our results have implications for the modeling and prediction of U.S. surface temperature anomalies during ENSO. Increasingly, such predictions are produced using dynamical models (e.g. Barnston et al. 2010). Whereas climate models have been

extensively validated as to their dynamical attributes regarding responses to ENSO (e.g. storm tracks, teleconnections), little is known about the fidelity of physical processes associated with the surface temperature response in models. It is evident from the results presented here that the latter is intimately tied to processes of water vapor, clouds, and surface properties, most of which require parameterization in atmospheric models. It is plausible to conceive, in fact likely to be the case, that different climate models may produce very similar teleconnection responses to ENSO forcing, yet render different U.S. surface temperature anomalies, either in amplitude and/or in pattern, owing to uncertainties in parameterizing the hydrologic cycle. In principle, our results suggest that accurate teleconnections will not guarantee accurate surface temperature signals (or predictions), to the extent that representation of key physical processes is deficient. In so far as ENSO is the primary source of U.S. surface temperature predictability, it is evident that a commensurate effort to evaluate the physics of temperature response be pursued to assess the suitability of climate model for such predictions as has previously been done for the dynamics of teleconnections (Kumar et al. 1996).

Our observational findings have presented a relatively detailed picture for understanding the physics of the U.S. surface temperature response to SST forcing, which may be useful for climate model validation used in seasonal forecasting, and may also serve as a stepping stone for understanding the U.S. surface temperature response to anthropogenic greenhouse gas forcing in nature and in models used for climate change projections.

## Acknowledgments

This research was supported by NOAA Climate Program Office. The leading author would like to thank Dr. Yuanchong Zhang for helpful discussions.

## References


Barnston, A., S. Li, S. Mason, D. DeWitt, L. Goddard, and X. Gong, 2010: Verification of the First 11 Years of IRI's Seasonal Climate Forecasts. *J. App. Met. And Clim*., 49, 493-520.

Chahine, M. T., 1992: The hydrological cycle and its influence on climate. *Nature,* 359, 373–380.

Held, I. M., S. W. Lyons, and S. Nigam, 1989: Transients and the extratropical response to El Niño. *J. Atmos. Sci.*, **46**, 163–174.

Hoerling, M. P. and M. Ting, 1994: On the organization of extratropical transients during El Niño. *J. Climate*, **7**, 745–766.

Hoerling M. P., A. Kumar, and M. Zhong, 1997: El Niño, La Niña, and the nonlinearity of their teleconnections. *J. Climate*, 10, 1769–1786.

Hoerling, M. P., and A. Kumar, 2000: Understanding and Predicting Extratropical Teleconnections Related to ENSO. Chapter 2 (pp 57-88) in "*El Niño and the Southern Oscillation: Multi-scale Variability, and Global and Regional Impacts* [eds. H. Diaz and V. Markgraf], Cambridge University Press, 496 pp.

Kiladis, G. N., and H. Diaz, 1989: Global climatic anomalies associated with extremes in the Southern Oscillation. *J. Climate,* **2,** 1069–1090.

Kumar, A., M. Hoerling, M. Ji, A. Leetmaa, and P. Sardeshmukh, 1996: Assessing a GCM's suitability for making seasonal predictions. *J. Climate*, **9**, 115–129.

Larkin, N. K., and D. E. Harrison, 2005: On the definition of El Niño and associated seasonal average U.S. weather anomalies, Geophys. Res. Lett., 32, L13705, doi:10.1029/2005GL022738.

Lau, N.C., A. Leetmaa, and M.J. Nath, 2008: Interactions between the Responses of North American Climate to El Niño–La Niña and to the Secular Warming Trend in the Indian–Western Pacific Oceans. *J. Climate*, **21**, 476–494.

May, W. and L. Bengtsson, 1998: The signature of ENSO in the Northen Hemisphere midlatitude seasonal mean flow and high-frequency intraseasonal variability. *Meteor. Atmos. Phys*, **69**, 81–100.

Mesinger F., Coauthors, 2006: North American Regional Reanalysis. *Bull. Amer. Meteor. Soc.*, 87, 343–360.

Quan, X., M. P. Hoerling, J. Whitaker, G. Bates, and T. Xu, 2006: Diagnosing sources of U.S. seasonal forecast skill. *J. Climate*, **19**, 3279-3293.

Ramanathan, V., P. J. Crutzen, J. T. Kiehl, and D. Rosenfeld, 2001: Aerosol, climate and the hydrological cycle, Science, 294, 2119–2124.

Ropelewski C. F., and M. S. Halpert, 1986: North American precipitation and temperature patterns associated with the El Niño/Southern Oscillation (ENSO). *Mon. Wea. Rev.*, 114, 2352–2362.

Ropelewski, C. F., and M. S. Halpert, 1987: Global and regional scale precipitation patterns associated with the El Niño/ Southern Oscillation. *Mon. Wea. Rev.,* **115,** 1606–1626.

Rossow, W. B., A. W. Walker, D. E. Beuschel, and M. D. Roiter, 1996: International Satellite Cloud Climatology Project (ISCCP) documentation of new cloud datasets, Rep. WMO/TD-737, 115 pp., World Meteorol. Organ., Geneva, Switzerland.

Soden B. J., 2000: The sensitivity of the tropical hydrological cycle to ENSO. *J. Climate*, 13, 538–549.

Sun, D.-Z., J. Fasullo, T. Zhang, and A. Roubicek, 2003: On the Radiative and Dynamical Feedbacks over the Equatorial Pacific Cold Tongue. *J. Climate*, 16, 2425–2432.

Sun, D.-Z., T. Zhang, C. Covey, S. Klein, W. Collins, J. Hack, J. Kiehl, G.A. Meehl, I.Held, and M. Suarez, 2006 : Radiative and Dynamical Feedbacks Over the Equatorial Cold-tongue: Results from Nine Atmospheric GCMs. *J. Climate* , 19, 4059-4074.

Sun, D.-Z., Y. Yu, and T. Zhang, 2009: Tropical Water Vapor and Cloud Feedbacks in Climate Models: A Further Assessment Using Coupled Simulations. *J. Climate*, **22**, 1287-1304.

Trenberth, K. E., G. W. Branstator, D. Karoly, A. Kumar, N.-C. Lau, and C. Ropelewski, 1998: Progress during TOGA in understanding and modeling global teleconnections associated with tropical sea surface temperatures, *J. Geophys. Res.*, 103(C7), 14,291–14,324.

Twomey, S. A., C. F. Bohren, and J. L. Mergenthaler. 1986: Reflectances and albedo differences between wet and dry surfaces. Appl. Opt., 25, 431–437.

Uppala, S. M., et al., 2005: The ERA-40 reanalysis, *Q. J. R. Meteorol. Soc*., 131, 2961–3012, doi:10.1256/qj.04.176/.

Wang, Z., C.P. Chang, and B. Wang, 2007: Impacts of El Niño and La Niña on the U.S. Climate during Northern Summer, *J. Climate*, **20**, 2165–2177.

Wild, M., A. Ohmura, H. Gilgen, and D. Rosenfeld, 2004: On the consistency of trends in radiation and temperature records and implications for the global hydrological cycle, *Geophys. Res. Lett.,* 31, L11201, doi:10.1029/2003GL019188.

Xie P. P, and P. A Arkin, 1997: Global precipitation: A 17-year monthly analysis based on gauge observations, satellite estimates, and numerical model outputs. *Bull. Amer. Meteor. Soc.*, 78, 2539–2558.

Yang F., A. Kumar, W. Wang, H.-M. H. Juang, and M. Kanamitsu, 2001: Snow–albedo feedback and seasonal climate variability over North America. *J. Climate*, **14**, 4245–4248.

Zhang, Y., W. B. Rossow, A. A. Lacis, V. Oinas, and M. I. Mishchenko, 2004: Calculation of radiative fluxes from the surface to top of atmosphere based on ISCCP and other global data sets: Refinements of the radiative transfer model and the input data, *J. Geophys. Res*., 109, D19105, doi:10.1029/2003JD004457.

Zhang, T., and D.-Z. Sun, 2006: Response of water vapor and clouds to El Niño warming in three National Center for Atmospheric Research atmospheric models, *J. Geophys. Res.*, 111, D17103, doi:10.1029/2005JD006700.

Zhang, T., and D.-Z. Sun, 2008: What causes the excessive response of clear-sky greenhouse effect to El Nino warming in Community Atmosphere Models? J. *Geophys. Res.,* 113, D02108, doi:10.1029/2007JD009247.

## Table captions

Table 1: List of warm and cold events from the observational datasets used in the composite analysis.

Table 2: The responses of surface temperature and the associated surface radiative fluxes averaged over the Pacific Northwest ($120^{O}$ W-$90^{O}$ W, $40^{O}$ N-$53^{O}$ N) and the Gulf Coast ($112^{O}$ W-$80^{O}$ W, $30^{O}$ N-$36^{O}$ N) for El Niño and over the Central U.S. ($120^{O}$ W-$90^{O}$ W, $37^{O}$ N-$45^{O}$ N) and the Gulf Coast ($112^{O}$ W-$80^{O}$ W, $30^{O}$ N-$36^{O}$ N) for La Niña. The meanings of symbols are below: "SFCT" indicates "surface temperature", "SRH" surface radiative heating, "LW_dn" downward surface longwave radiation, "SW_dn" downward surface solar radiation, "SW_up" upward surface solar radiation, "SW_net" absorbed solar radiation at surface. Note that here SRH = LW_dn + SW_net = LW_dn + SW_dn +SW_up.

## Figure captions

Figure 1**:** Composites of seasonally averaged DJF (December to February) surface temperature anomalies for (a) El Niño and (b) La Niña events. See Table 1 (section 2) for the years used in the composites. Units are $^{O}$C.

Figure 2: The composite DJF anomalies of (a) upward longwave radiation, (b) surface radiative heating, (c) net radiation, and (d) the turbulent fluxes for El Niño events. (e–h) Corresponding anomalies of surface energy flux for La Niña events. Units are $W/m^2$. The surface radiative heating is defined as the sum of the absorbed shortwave and downward longwave radiation at the surface. The net radiation is equal to the sum of surface radiative heating and the upward longwave radiation. The turbulent fluxes are the sum of latent heat flux (LH) and sensible heat flux (SH). Note that energy gain for the surface is signed positive, and energy loss for the surface is signed negative, and provide qualitative indication of their contributions to surface temperature tendency.

Figure 3: The composite DJF anomalies of (a) absorbed shortwave radiation at surface, (b) surface upward shortwave flux, (c) surface downward shortwave flux, (d) cloud optical thickness for El Niño events. (e–h) Corresponding anomalies for La Niña events. Units for radiative fluxes are $W/m^2$ and Units for cloud optical thickness are dimensionless.

Figure 4: The composite DJF anomalies of (a) surface albedo, (b) snow cover, (c) soil moisture content, and (d) precipitation for El Niño events. (e–h) Corresponding anomalies for La Niña events. Units for surface albedo are dimensionless and those for snow cover, soil moisture content and precipitation are %, $Kg/m^2$, and mm/day, respectively.

Figure 5: The composite DJF anomalies of (a) downward longwave radiation at surface, and (b) total column precipitable water for El Niño events. (c–d) Corresponding anomalies for La Niña events. Units for radiative fluxes are $W/m^2$ and those for precipitable water are $Kg/m^2$.

Figure 6: Schematic diagram showing the physical mechanisms by which the water vapor, clouds, and surface properties (indicated by surface albedo) determine the wintertime surface temperature over the continental United States during ENSO events. Note that contributions to surface warming (cooling) are plotted in red (blue) for water vapor and clouds, and are plotted in black (white) for surface albedo. Reduced surface albedo is indicated by dark shades implying darker surface conditions contributing to warming.

**Table 1. List of warm and cold events from the observational datasets used in the composite analysis.**

| Variable (Symbol) | Dataset | Warm events | Cold events | Reference |
|---|---|---|---|---|
| Surface radiative fluxes | ISCCP FD | 1986/87; 1987/88; 1991/92; 1994/95; 1997/98; 2002/03 | 1988/89; 1995/96; 1998/99; 1999/2000 | Zhang et al. (2004) |
| Surface temperature, surface albedo and total column precipitable water | ISCCP FD | same as above | same as above | same as above |
| cloud amount and cloud optical thickness | ISCCP D2 | 1986/87; 1987/88; 1991/92; 1994/95; 1997/98; 2002/03 | 1988/89; 1995/96; 1998/99; 1999/2000 | Rossow et al. (1996) |
| Precipitation | CMAP | 1982/83; 1986/87; 1987/88; 1991/92; 1994/95; 1997/98; 2002/03 | 1988/89; 1995/96; 1998/99; 1999/2000 | Xie and Arkin (1997) |
| Surface latent and sensible heat fluxes (LH and SH) | ERA-40 reanalysis | 1986/87; 1987/88; 1991/92; 1994/95; 1997/98 | 1988/89; 1995/96; 1998/99; 1999/2000 | Uppala et al. (2005) |
| Snow cover and soil moisture content | NARR data | 1982/83; 1986/87; 1987/88; 1991/92; 1994/95; 1997/98; 2002/03 | 1988/89; 1995/96; 1998/99; 1999/2000 | Mesinger et al. (2006) |

ISCCP = International Satellite Cloud climatology Project.
CMAP = CPC Merged Analysis of Precipitation.
ERA-40 = 40-yr ECMWF Re-Analysis.
NARR = North American Regional Reanalysis.

Table 2: The responses of surface temperature and the associated surface radiative fluxes averaged over the Pacific Northwest ($120^O$ W-$90^O$ W, $40^O$ N-$53^O$ N) and the Gulf Coast ($112^O$ W-$80^O$ W, $30^O$ N-$36^O$ N) for El Niño and over the Central U.S. ($120^O$ W-$90^O$ W, $37^O$ N-$45^O$ N) and the Gulf Coast ($112^O$ W-$80^O$ W, $30^O$ N-$36^O$ N) for La Niña. The meanings of symbols are below: "SFCT" indicates "surface temperature", "SRH" surface radiative heating, "LW_dn" downward surface longwave radiation, "SW_dn" downward surface solar radiation, "SW_up" upward surface solar radiation, "SW_net" absorbed solar radiation at surface. Note that here SRH = LW_dn + SW_net = LW_dn + SW_dn +SW_up.

| Responses to ENSO | El Niño | | La Niña | |
|---|---|---|---|---|
| | Pacific Northwest | Gulf Coast | Central U.S. | Gulf Coast |
| SFCT ($^O$C) | 1.6 | -0.6 | 2.0 | 1.4 |
| | | | | |
| SRH ($W/m^2$) | 8.7 | -1.7 | 5.6 | 10.1 |
| LW_dn ($W/m^2$) | 4.9 | 1.9 | 2.2 | 3.7 |
| SW_dn ($W/m^2$) | 0.2 | -3.6 | -1.7 | 5.1 |
| SW_up ($W/m^2$) | 3.6 | 0.0 | 5.1 | 1.4 |
| SW_net ($W/m^2$) | 3.8 | -3.6 | 3.5 | 6.4 |

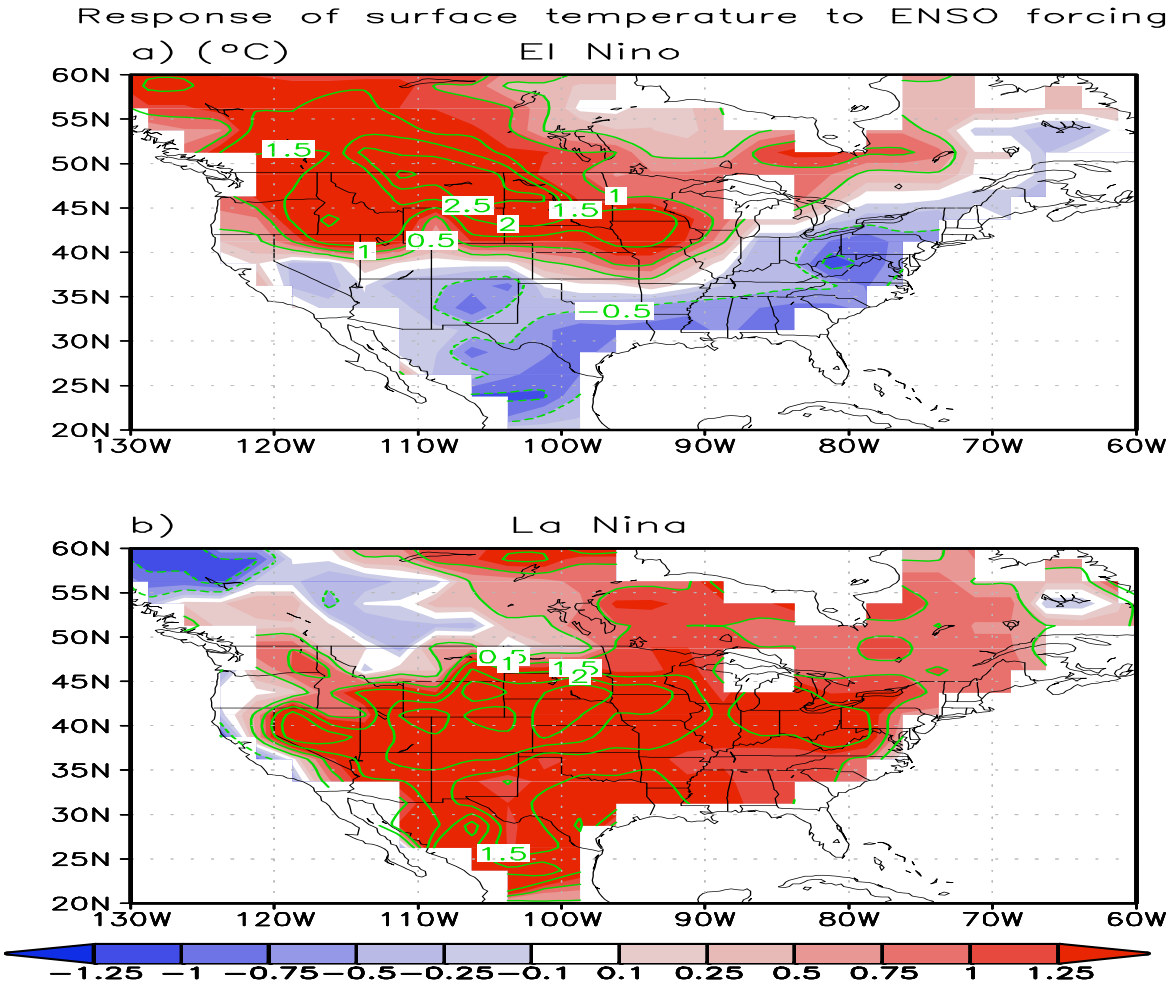


Figure 1: Composites of seasonally averaged DJF (December to February) surface temperature anomalies for (a) El Niño and (b) La Niña events. See Table 1 (section 2) for the years used in the composites. Units are $^{o}$C.

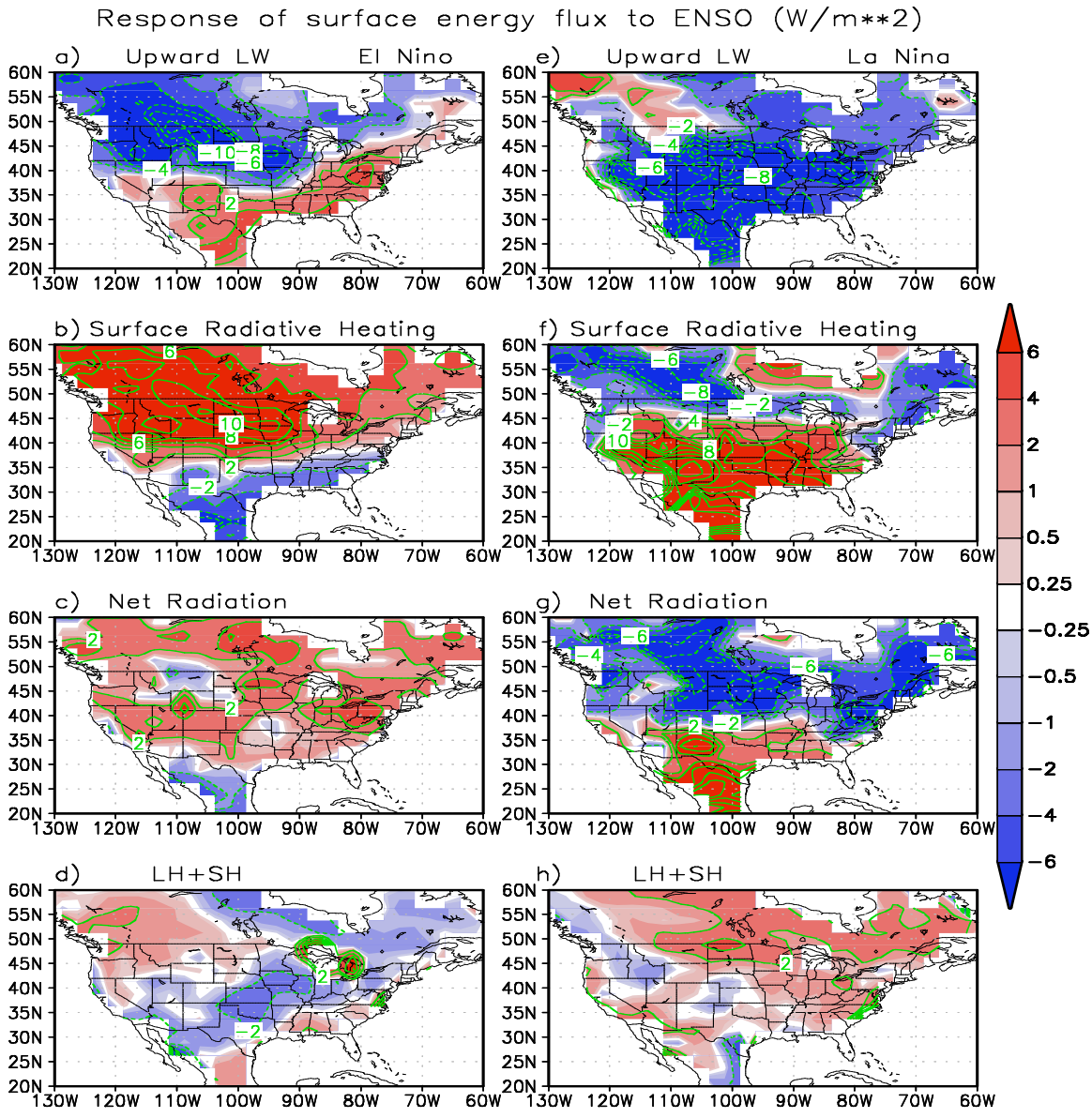


Figure 2: The composite DJF anomalies of (a) upward longwave radiation, (b) surface radiative heating, (c) net radiation, and (d) the turbulent fluxes for El Niño events. (e–h) Corresponding anomalies of surface energy flux for La Niña events. Units are W/m$^2$. The surface radiative heating is defined as the sum of the absorbed shortwave and downward longwave radiation at the surface. The net radiation is equal to the sum of surface radiative heating and the upward longwave radiation. The turbulent fluxes are the sum of latent heat flux (LH) and sensible heat flux (SH). Note that energy gain for the surface is signed positive, and energy loss for the surface is signed negative, and provide qualitative indication of their contributions to surface temperature tendency.

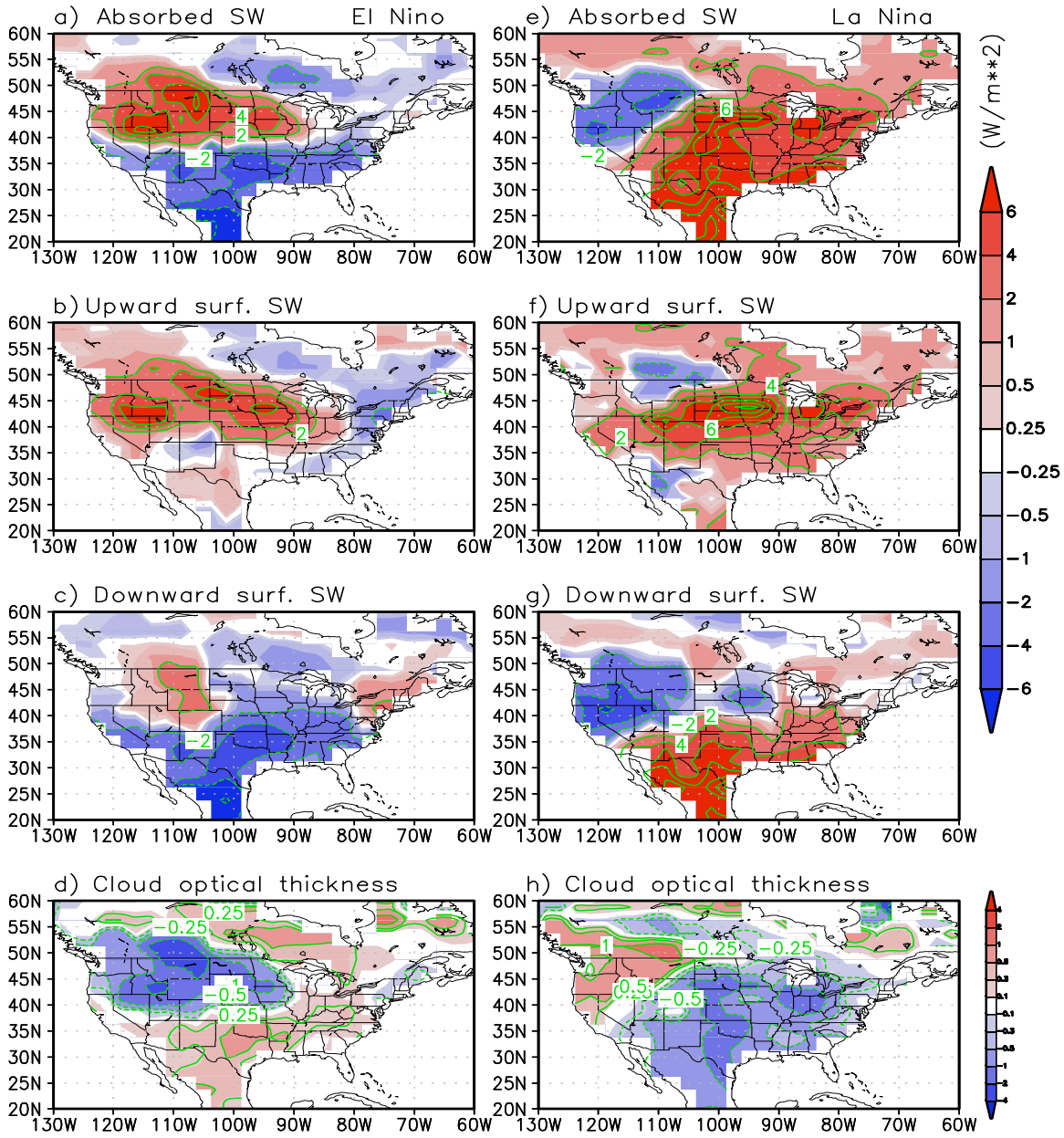


Figure 3: The composite DJF anomalies of (a) absorbed shortwave radiation at surface, (b) surface upward shortwave flux, (c) surface downward shortwave flux, (d) cloud optical thickness for El Niño events. (e–h) Corresponding anomalies for La Niña events. Units for radiative fluxes are W/m$^2$ and Units for cloud optical thickness are dimensionless.

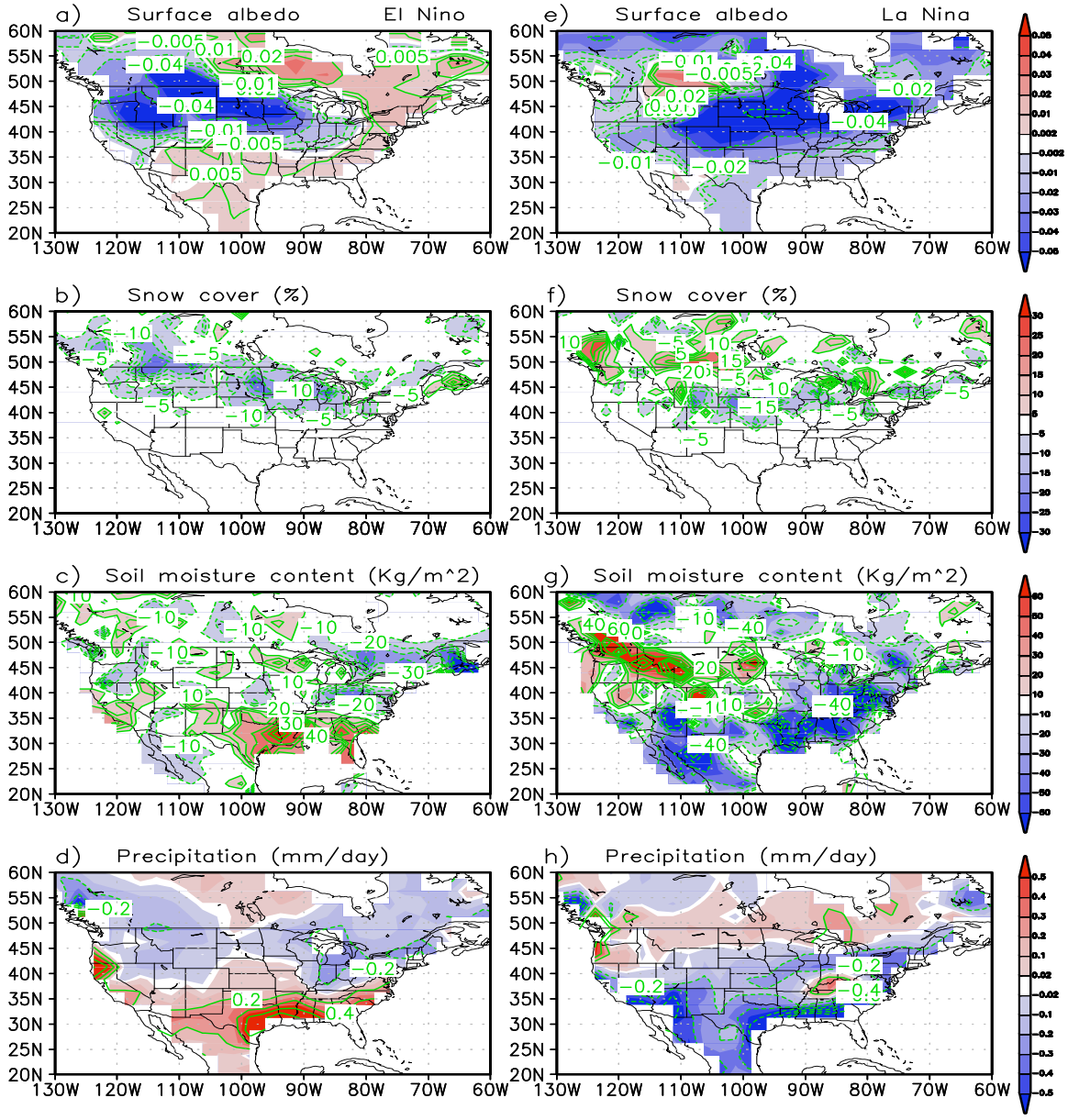


Figure 4: The composite DJF anomalies of (a) surface albedo, (b) snow cover, (c) soil moisture content, and (d) precipitation for El Niño events. (e–h) Corresponding anomalies for La Niña events. Units for surface albedo are dimensionless and those for snow cover, soil moisture content and precipitation are %, Kg/m$^2$, and mm/day, respectively.

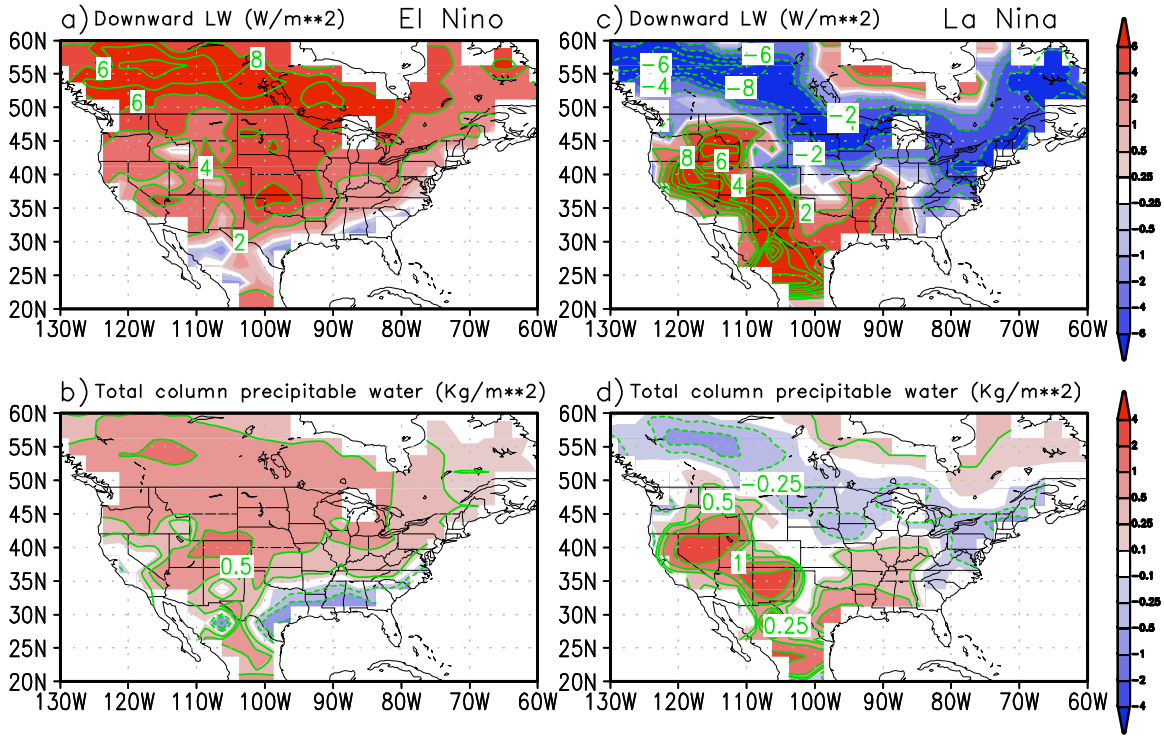


Figure 5: The composite DJF anomalies of (a) downward longwave radiation at surface, and (b) total column precipitable water for El Niño events. (c–d) Corresponding anomalies for La Niña events. Units for radiative fluxes are $W/m^2$ and those for precipitable water are $Kg/m^2$.

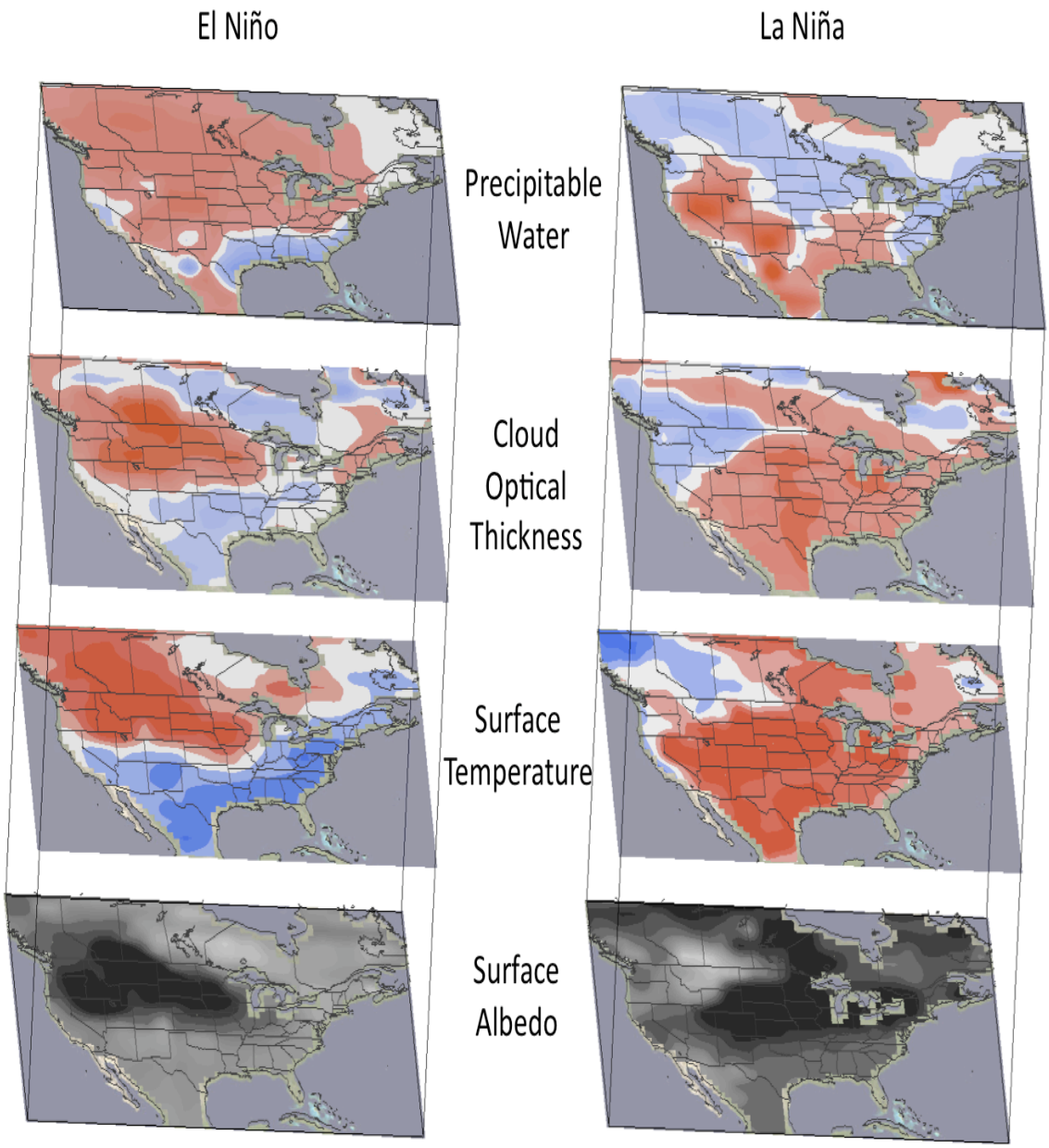


Figure 6: Schematic diagram showing the physical mechanisms by which the water vapor, clouds, and surface properties (indicated by surface albedo) determine the wintertime surface temperature over the continental United States during ENSO events. Note that contributions to surface warming (cooling) are plotted in red (blue) for water vapor and clouds, and are plotted in black (white) for surface albedo. Reduced surface albedo is indicated by dark shades implying darker surface conditions contributing to warming.